Tuning the morphology and optical properties of one-dimensional Ag nanomaterials via anodic aluminum oxide template

XUE WEI WANG[*,a,b], ZHAO CHENG HE[a], TIAN YI WANG[a], ZHI HAO YUAN[a,c]
[a]*School of Materials Science & Engineering, Tianjin University of Technology, Tianjin 300384, People's Republic of China*
[b]*Tianjin Key Lab for Photoelectric Materials and Devices, Tianjin 300384, People's Republic of China*
[c]*Key Laboratory of Display Materials & Photoelectric Devices (Tianjin University of Technology), Ministry of Education, Tianjin 300384, People's Republic of China*

One-dimensional Ag nanomaterials with different shapes have been prepared using direct-current electrodeposition within the confined nanochannels of the anodic aluminum oxide templates. The morphologies and crystal structures of the straight, Y-shaped and graded Ag nanowires are observed by field-emission scanning electron microscopy, transmission electron microscopy, and X-ray diffractometer. Absorption spectra of Ag nanowires dispersed in the ethanol are measured to reveal the relation between the morphology and the optical properties. The results indicate that the graded Ag nanowires have the higher broad band optical absorption efficiency because the diameter of the graded Ag nanowires continuously changes from 21 nm to 44 nm. These findings provide a viable and convenient route for designing shape-controlled nanowire-based high-performance photonic devices by the surface plasmon resonance of nanostructures.

(Received December 22, 2012; accepted March 13, 2014)

Keywords: Nanowires, Template synthesis, Electrodeposition, Optical absorption

1. Introduction

Recently, the fabrication of shape-selective metal nanostructures has attracted continuous interest because of their unique physical and chemical properties and broad applications in catalysis, electronics, and plasmonics and so on [1-7]. Especially, the noble metal nanostructure systems exhibit strong optical absorption at visible and ultraviolet wavelength with wide usage due to the surface plasmon resonance (SPR), which is the collective resonant absorption of free electrons at the surface of metal nanostructures. Up to now, various approaches have been developed to generate the noble metal nanostructures, which include zero-dimensional spherical or tetrahedral nanoparticles [8-10], one-dimensional nanorods and nanowires [11-13], and two-dimensional nanoplates [14-16]. Among these nanostructures, Ag nanowires with large length-to-diameter ratios exhibit promising properties for applications in flexible thin-film electrodes [17-19], surface-enhanced Raman scattering (SERS) active substrates [20-22], functional nanocomposites [23-25], controllable plasmon routers [26]. It is well known that the properties of nanomaterials are determined by their dimensions, geometry, and crystallinity [27]. As a result, in order to tune the optical properties and realize the application in optical devices, it is a challenge for us to control the morphology of Ag nanowires.

Among the various methods which have been used to fabricate the nanolevel architectures with good shape control, the template-assisted method is one of the widely investigated and exploited approaches because of its own advantages, such as precisely controlling the morphology and dimension of the nanostructures. For the template materials, porous anodic aluminum oxide (AAO) has wide range of adjustable pore diameters (10-250 nm), high pore density (up to 10^{10} cm^{-2}) and controllable channel lengths [28]. More importantly, the AAO template, which prepared by an anodic oxidation of aluminum under appropriate electrolyte solutions and anodizing voltages, is typical self-ordered nanoporous structures including straight, Y-shaped, graded pores. In this paper, the straight, Y-shaped and graded Ag nanowires are fabricated within the confined nanochannels of the AAO templates. By analysing the optical properties of Ag nanowires, it can be obtained the relation between the SPR of the nanowires and the morphology. The correlative research will provide useful

reference for applications utilizing plasmon resonance of the noble metal nanostructures.

2. Experimental

The AAO templates are prepared using a two-step anodization process as described previously [28]. In this experiment, we modify the procedure to obtain the pores of AAO templates with different shapes. Briefly, prior to anodizing, high-purity aluminum foils (99.999%) are annealed in a vacuum of 10^{-3} Pa at 500 ºC for 5 h to remove the mechanical stress and obtain homogenous conditions for pore growth over a large area. For the first anodization, the high-purity aluminum foils are anodized in the acid solutions of 0.3 M oxalic acid and 0.3 M sulfuric acid under the potential of 40 V and 24 V at the temperature of 5 ºC, respectively. Before the second anodization, the previous AAO membrane is removed in a mixture of phosphoric acid (6 wt%) and chromic acid (1.8 wt%) at 60 °C. For the AAO template with straight pores, the second anodization is performed in the acid solutions of 0.3 M sulfuric acid under the potential of 24 V. For the AAO template with graded pores, the high-purity aluminum foils are anodized again in 0.3 M oxalic acid under a gradually decreasing the voltage from 40 V to 20 V. During the second-step anodization, the AAO template with graded pore diameter is formed because its pore diameter is proportional to the voltage. For the AAO template with Y-shaped pores, the high-purity aluminum foils is anodized in 0.3 M oxalic acid under the potential of 40 V for 6 h, and followed by abruptly decreasing the voltage to 28 V. Then Y-shaped pores are formed at the change of the voltage. After the second anodization, all AAO templates are etched by saturated $CuCl_2$ solution to remove the remaining aluminum. The alumina barrier layer is then dissolved in 5 wt% H_3PO_4 solution at 30 ºC. Finally, a layer of Au film is sputtered onto one side of the AAO template to serve as the working electrode in a two-electrode plating cell, and a graphite plate is used as the counter electrode. The corresponding electrolyte is a mixture of 45 g/L $AgNO_3$ and 40 g/L H_3BO_3 in aqueous solutions, and the pH value of the solution is adjusted to the range of 2~3 by adding H_3NO_3 solution.

The crystal structures of Ag nanowire arrays are characterized by X-ray diffractometer (Rigaku D/MAX2500) with Cu $K\alpha_1$ radiation (λ=0.154056 nm). The morphologies of Ag nanowires with different shapes are observed with field-emission scanning electron microscopy (FE-SEM: JEOL JSM-6700F) and transmission electron microscopy (TEM: JEOL JEM-2100). For X-ray diffraction (XRD) measurements, the overfilled nanowires on the surface of the AAO template are mechanically polished away using super-fine alumina powders. For scanning electron microscopy observations, the AAO is partly dissolved with 0.5 M NaOH solution, and then carefully rinsed with deionized water for several times. For transmission electron microscopy observations, the AAO is completely dissolved with 1 M NaOH solution and then rinsed with absolute ethanol. Then the ethanol solutions of the as-prepared silver nanowires are cast onto carbon-coated copper grids and dried naturally. Absorbance spectra of the samples are performed with UV-Visible spectrophotometer (TU-1901). Ag nanowires with different shapes are dispersed in ethanol solution during the measurement of the absorption spectra.

3. Results and discussion

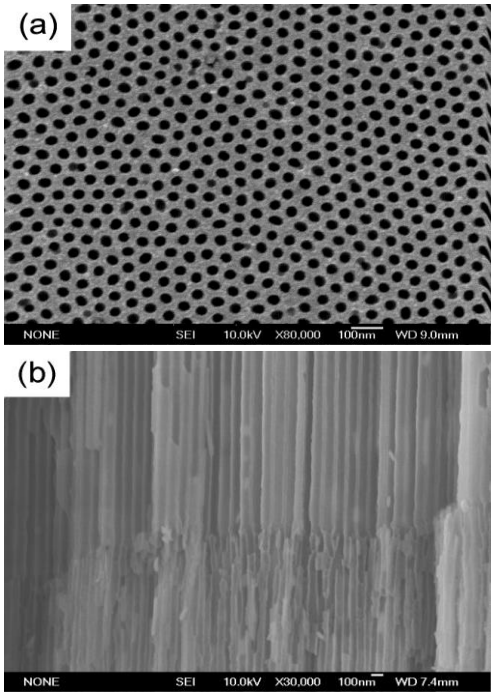

Fig. 1. FE-SEM images of AAO templates: (a) the top view of AAO template with straight pores; (b) the side view of AAO template with Y-shaped pores.

The morphologies of the as-prepared AAO templates are shown in Fig. 1. Fig. 1(a) is a typical top view FE-SEM image of as-prepared AAO template with straight pores. It can be seen that the AAO has highly order hole arrangement with an average diameter of about 25 nm. Fig. 1(b) is the typical side view image of AAO template with Y-shaped pores. It can be seen from Fig. 1(b) that two kinds of pore diameters are shown along the pores, which is anodized under the voltage of 40V and 28V respectively. There is Y-shaped hole structure at the conversion of the anodizing voltage.

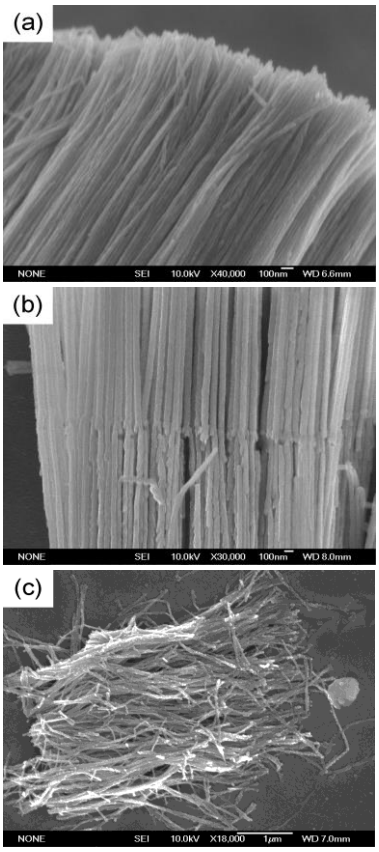

Fig. 2. FE-SEM images of Ag nanowires with different shapes: (a) the straight; (b) the Y-shape; (c) the graded shape.

Fig. 2 shows FE-SEM images of Ag nanowires with different shapes which are liberated from the AAO template. It can be seen from Fig. 2(a) that Ag nanowires have the uniform diameter because of the finite effects of the pores of the AAO. As shown in Fig. 2(b), Ag nanowires with the Y-shaped structure are completely liberated from the AAO template. The low-magnification FE-SEM image of the graded Ag nanowires is shown in Fig. 2(c), and indicates that a large amount of the graded Ag nanowires are released from the pores of the AAO template.

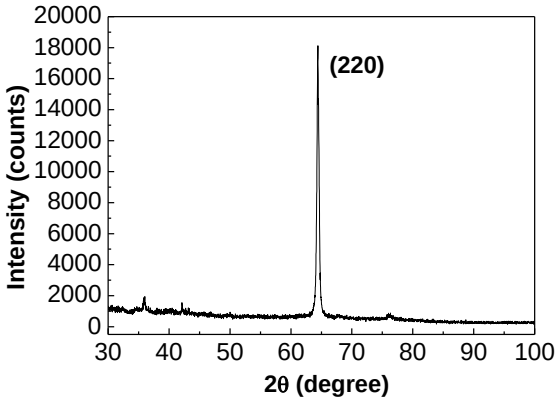

Fig. 3. XRD pattern of Ag nanowire array.

In Fig. 3, it is shown the XRD pattern of Ag nanowires with the uniform diameter. The XRD pattern is taken from the top side of the samples after polishing. The peak with the most intensity can be readily indexed to (220) plane of the face-centered cubic (FCC) structure according to the standard diffraction peaks of Ag (JCPDS 04-0783), which indicates that Ag nanowires are well crystallized and successfully synthesized by the electrodeposition method. The intensity for (220) planes is very strong and higher than the others, which shows that Ag nanowires have a preferred orientation along the [110] direction during the growing of the nanowires. Moreover, we have checked XRD patterns of Ag nanowires with different shapes and find that they have the same FCC structure and the preferred orientation.

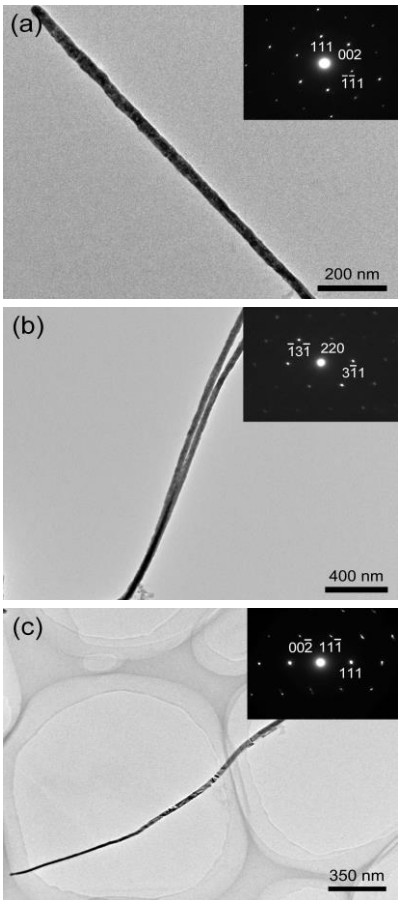

Fig. 4. TEM images and SAED patterns of Ag nanowires with different shapes: (a) the straight; (b) the Y-shape; (c) the graded shape.

TEM images and selected-area electron diffraction (SAED) patterns are performed to further confirm the structure and morphology of Ag nanowires. It is clear that the nanowire has a high-aspect ratio, and the diameter is uniform in Fig. 4(a). The diameter of nanowires is restricted by the diameter of pores of the AAO, and is about 25 nm. It can be seen from the inset of Fig. 4(a) that the diffraction pattern contains a set of

diffraction spots which can be assigned to FCC structure, indicating that Ag nanowires have a single crystal structure. Fig. 4(b) shows a typical TEM image of a single Ag nanowire with Y-shape. For Y-shaped Ag nanowire, the diameter of trunk is about 55 nm, while the diameter of embranchment is about 30 nm. According to SAED pattern in the inset of Fig. 4(b), it is found that the structure of the nanowire is also FCC. In Fig. 4(c), it is shown a typical TEM image of a single Ag nanowire with the graded diameter, and the diffraction pattern can be indexed to FCC structure. One can see that the diameter of Ag nanowire changes from 21 nm to 44 nm in Fig. 4(c).

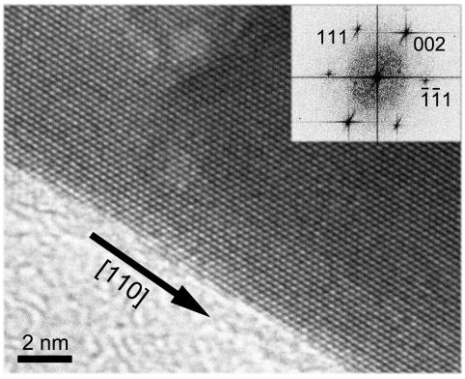

Fig. 5. HRTEM image and the corresponding FFT pattern of Ag nanowires with the diameter of 25 nm.

To further confirm the growth orientation of Ag nnanowires, the lattice fringes of the nanowire are investigated by the high-resolution TEM (HRTEM). The corresponding image is shown in Fig. 5. It can be seen from the lattice fringes and the corresponding fast fourier transform (FFT) shown in the inset of Fig.5 that FCC Ag nanowire is the single-crystalline and has a preferred orientation along the [110] direction. The HRTEM analysis is in accord with the result of XRD shown in Fig. 3.

For noble metal nanomaterials, the excitation of surface plasmon by an electric field (light) at a wavelength results in the appearance of intense absorption bands. Fig. 6 presents the absorption spectra of Ag nanowires with different shapes in ethanol solution. For the Ag nanowires with the diameter of 25 nm, there is one sharp-band absorption from approximately 344 nm to 424 nm which corresponds to the SPR absorption associated with the short axis of Ag nanowires. The center of the strong and sharp absorption peak is at 371 nm. For Y-shaped Ag nanowires, this spectrum displays a dual peak line shape, and the center positions of the two peaks are at 390 nm and 400 nm respectively. The two peaks can be ascribed to the embranchment resonance absorption and the trunk resonance absorption of Y-shaped Ag nanowires, respectively. At the same time, the spectral position of two absorption peaks exhibits a distinct red shifting comparing with the absorption peak of the Ag nanowires with the diameter of 25 nm. However, for the graded Ag nanowires, a broad absorption peak appears in the range from 340 nm to 660 nm and the center of the absorption peak is at 377 nm. Because the diameter of the graded Ag nanowires ranges from 21 nm to 44 nm, and continuously changes, the absorption peak has the broader range compared with the absorption peaks for the diameter of 25 nm and Y-shape of Ag nanowires. According to these results, we know that the size and shape of Ag nanowires are some of the most powerful handles for controlling and manipulating the plasmonic response of these materials, and play some of the key roles in determining the positions of SPR resonance mode.

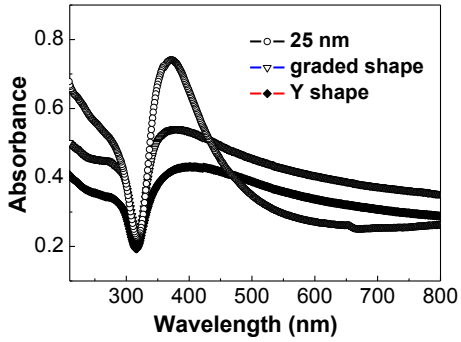

Fig. 6. UV-visible absorption spectra of Ag nanowires with different shapes dispersed in the ethanol.

4. Conclusion

In summary, Ag nanowires with controllable shape and size have been fabricated by direct-current electrodeposition in the pores of AAO templates. The results of XRD and TEM show that Ag nanowires are the FCC structure and have a preferred orientation along the [110] direction. For Ag nanowires with the diameter of 25 nm, one sharp-band absorption from approximately 344 nm to 424 nm, the center of the strong and sharp absorption peak is at 371 nm. For Y-shaped Ag nanowires, this spectrum displays a dual peak line shape, and the center positions of the two peaks are at 390 nm and 400 nm respectively. While, for the graded Ag nanowires, a broad absorption peak appears in the range from 340 nm to 660 nm and the center of the absorption peak is at 377 nm. These results indicate that the plasmonic properties of Ag nanowires have been controlled by tuning the morphological parameters.

Acknowledgements

This work is supported by the National Natural Science Foundation of China (No. 10904108 and 21171128) and Tianjin Key Subject for Materials Physics and Chemistry.

References

[1] W. Wei, S. Li, L. Qin, C. Xue, J. E. Millstone, X. Xu, G. C. Schatz, C. A. Mirkin, Nano Lett., **8**, 3446 (2008).

[2] S. Mahima, R. Kannan, I. Komath, M. Aslam, V. K. Pillai, Chem. Mater., **20**, 601 (2008).

[3] J. Yao, Z. Liu, Y. Liu, Y. Wang, C. Sun, G. Bartal, A. M. Stacy, X. Zhang, Science, **321**, 930 (2008).

[4] W. Y. Li, P. H. C. Camargo, X. M. Lu, Y. N. Xia, Nano Lett., **9**, 485 (2009).

[5] R. Gunawidjaja, E. Kharlampieva, I. Choi, V. V. Tsukruk, Small, **5**, 2460 (2009).

[6] Y. P. Bi, H. Y. Hu, G. X. Lu, Chem. Commun., **46**, 598 (2010).

[7] L. Yi, X. Zhou, Y. Fu, L. Yang, Plasmonics, **6**, 281 (2011).

[8] Z. L. Wang, S. A. Harfenist, I. Vezmar, R. L. Whetten, J. Bentley, N. D. Evans, K. N. Alexander, Adv. Mater., **10**, 808 (1998).

[9] H. G. Svavarsson, J. W. Yoon, S. H. Song, R. Magnusson, Plasmonics, **6**, 741 (2011).

[10] Q. Wang, F. Song, S. Lin, C. Ming, H. Zhao, J. Liu, C. Zhang, E. Y. B. Pun, J. Nanopart. Res., **13**, 3861 (2011).

[11] Y. Zhou, S. H. Yu, C. Y. Wang, X. G. Li, Y. R. Zhu, Z. Y. Chen, Adv. Mater., **11,** 850 (1999).

[12] S. Liu, J. Yue, A.Gedanken, Adv. Mater., **13**, 656 (2001).

[13] Y. Tsutsui, T. Hayakawa, G. Kawamura, M. Nogami, Nanotechnology, **22**, 275203 (2011).

[14] X. Q. Cui, C. M. Li, H. F. Bao, X. T. Zheng, J. F. Zang, C. P. Ooi, J. Guo, J. Phys. Chem. C, **112**, 10730 (2008).

[15] G. Q. Liu, W. P. Cai, C. H. Liang, Crystal Growth and Design, **8**, 2748 (2008).

[16] B. H. Lee, M. S. Hsu, Y. C. Hsu, C. W. Lo, C. L. Huang, J. Phys. Chem. C, **114**, 6222 (2010).

[17] B. E. Hardin, W. Gaynor, I-K Ding, S-B Rim, P. Peumans, M. D. McGehee, Organic Electronics, **12**, 875 (2011).

[18] J. Y. Lee, S. T. Connor, Y. Cui, Nano Lett., **8**, 689 (2008).

[19] X. Y. Zeng, Q. K. Zhang, R. M. Yu, C. Z. Lu, Adv. Mater., **22**, 4484 (2010).

[20] S. B. Chaney, S. Shanmukh, R. A. Dluhy, Y. P. Zhao, Appl. Phys. Lett., **87**, 031908 (2005).

[21] C. L. Du, Y. M. You, T. Chen, Y. Zhu, H. L. Hu, D. N. Shi, H. Y. Chen, Z. X. Shen, Plasmonics, **6**, 761 (2011).

[22] C. Zhao, S. L. Tang, Y. W. Du, Chem. Phys. Lett., **491**, 183 (2010).

[23] R. Gunawidjaja, C. Y. Jiang, H. H. Ko, V. V. Tsukruk, Adv. Mater., **18**, 2895 (2006).

[24] R. Gunawidjaja, C. Y. Jiang, S. Peleshanko, M. Ornatska, S. Singamaneni, V. V. Tsukruk, Adv. Funct. Mater., **16**, 2024 (2006).

[25] R. Gunawidjaja, H. Ko, C. Y. Jiang, V. V. Tsukruk, Chem. Mater., **19**, 2007 (2007).

[26] Y. Fang, Z. Li, Y. Huang, S. Zhang, P. Nordlander, N. J. Halas, H. Xu, Nano Lett., **10**, 1950 (2010).

[27] X. G. Peng, L. Manna, W. D. Yang, J. Wickham, E. Scher, A. Kadavanich, A. P. Alivisatos, Nature, **404**, 59 (2000).

[28] A. P. Li, F. Müller, A. Birner, K. Nielsch, U.Gösele, J. Appl. Phys., **84**, 6023 (1998).

*Corresponding author: xwwang@tjut.edu.cn